# Towards Enhanced Reliability of Active Distribution Systems with Adaptive Control of Inverters

Hadis Hosseinpour, Student Member, IEEE, Mohammed Benidris, Senior Member, IEEE, and Joydeep Mitra, Fellow, IEEE

Department of Electrical and Computer Engineering, Michigan State University, East Lansing, MI 48824 Emails: hossei13@msu.edu, benidris@msu.edu, mitraj@msu.edu

Abstract—Electricity distribution companies are actively working to improve grid operational efficiency and reliability to meet the evolving expectations of customers. Achieving these objectives necessitates the utilization of advanced control methods for distributed power generation while emphasizing grid reliability improvements. This paper proposes an approach to integrate adaptive control systems of inverter-based resources (IBRs) with reliability evaluation of distribution systems to improve the impact of IBRs on overall system reliability. This approach effectively utilizes adaptive droop control of inverter-based distributed energy resources, leading to substantial enhancements in system reliability. The proposed approach leverages mixed-integer linear programming optimization and incorporates detailed linear AC optimal power flow to find efficient solutions. Notably, this study is pioneering in its incorporation of adaptive droop control into reliability assessments, demonstrating significant improvements in critical reliability indicators like the System Average Interruption Duration and Frequency Indices (SAIDI) and (SAIFI) in distribution systems. The effectiveness of the proposed approach is validated through a series of diverse case studies conducted on the IEEE 33-bus test system.

Index Terms—Reliability assessment, adaptive control, active distribution system, droop control, inverter-based resources.

#### I. INTRODUCTION

Reliability assessment of distribution systems is crucial for ensuring consistent electricity delivery with acceptable power quality. This is essential for residential, commercial, and industrial consumers. The integration of inverter-based distributed generation has been increasing for eco-friendly and cost-effective networks. However, this integration requires efficient operational strategies to maximize generation resource potential, especially during failures and unpredictable weather. Therefore, a comprehensive examination of distribution systems is needed to address these complex challenges.

This research investigates the impact of *adaptive control systems* of inverters on the *reliability assessment* of distribution systems, such that the role of adaptive droop control in maximizing the potential of inverters to support the overall system's reliability is studied. The adaptive control system for inverter-based resources (IBRs) plays a pivotal role in providing more flexibility in the operating points of IBRs and improving the ability of the distribution grid to maintain reliability and power quality.

The complexity of distribution systems with renewable energy sources (RESs) and their potential operational challenges are being taken into consideration, including the various modes

of microgrid operation [1]–[5], the customer impacts [6], [7], the uncertainty of RESs [1], [8], integrating transient stability and reliability assessment of RESs [9], and the impact of microgrid penetration in the distribution system as well as main utility and their reliability [10]–[12]. Most of exciting studies have considered IBRs as dispatchable units that cannot represent the accurate inverter operation model. On the other hand, by modeling the inverters using the traditional droop control, the operation of the IBRs as a small autonomous unit to help improve system reliability, can be limited.

Therefore, the high penetration of IBRs requires a focus on utilizing more intelligent and advanced control of inverters to unlock their potential to improve the reliability of distribution systems. Also, it is necessary to incorporate IBRs and an intelligent control system that can be modified based on grid state in the reliability studies of an active distribution system. The capability of the IBRs should be modeled such that after each contingency, the system can utilize the most possible power generated by IBRs. Moreover, the interdependency of load and inverter droop control with voltage and power needs to be considered. By accurately representing the models of IBRs, loads, and power flow while taking into account the interdependency between voltage and reactive power, the reliability assessment can unveil the latent potential of adaptive droop control in IBRs as well as reactive power and voltage regulation to enhance the overall system reliability.

This paper integrates adaptive control techniques with the assessment of system reliability. It achieves this by implementing a meticulous linear optimization framework, taking into account inverter controls, adaptive control systems for inverters, and voltage-dependent load models. A precise and comprehensive linear AC optimal power flow (AC-OPF) approach is employed to facilitate the evaluation of sequential Monte Carlo reliability assessments. Furthermore, the inclusion of the ZIP load model for load characterization, along with its application to inverters, enables the fine-tuning of voltage regulation in both normal operating conditions and contingency scenarios. The main contributions of this paper are as follows:

- The proposed approach bridges the gap between reliability assessment and inverter control system in distribution systems in under a mixed-integer linear programming (MILP) optimization framework.
- An intelligent droop control scheme is proposed to fully optimize the potential of IBRs for enhanced reliability.

 A comprehensive numerical assessment under sequential Monte Carlo simulation with detailed modeling of linear AC-OPF, adaptive droop control of inverters, and the ZIP load model is presented.

The rest of the paper is organized as follows. Section II formulates the MILP problem. In Sections III and IV, the proposed approach is simulated, analyzed, and concluded.

#### II. METHODOLOGY AND MODELING

#### A. Linear AC Optimal Power Flow

This study focuses on the importance of considering voltage and reactive power dependency in distribution system reliability studies. To simulate this dependency, the paper proposes the use of the AC-OPF model, which can provide a more realistic assessment of distribution system reliability for the interdependency of voltage and reactive power. By optimizing these variables, AC-OPF provides a more comprehensive framework for ensuring the efficient and stable operation of the power distribution system. However, the nonlinear AC-OPF model is computationally intensive and time-consuming, especially when conducting reliability studies that require multiple power flow analyses. To overcome this limitation and improve the efficiency of reliability assessments, this paper introduces a linear AC-OPF model, which is expected to strike a balance between accuracy and computational complexity [13]. The subsequent section of the paper elaborates on the development of this linear AC-OPF model. At each node i, the general equations for power flow can be written as follows:

$$P_i^{\text{sub}} + P_i^{\text{IBR}} = P_i^{\text{L}} + \sum_{j=1}^{\eta} P_{ij}^{\text{line}}, \ Q_i^{\text{sub}} + Q_i^{\text{IBR}} = Q_i^{\text{L}} + \sum_{j=1}^{\eta} Q_{ij}^{\text{line}}.$$
 (1)

where  $\eta$  is the number of nodes;  $(.)_i^{\mathrm{sub}}$  denotes the power supplied by the substation at node i in p.u.;  $(.)_i^{\mathrm{IBR}}$  represents power generations by the IBR at node i in p.u.; and  $(.)_i^{\mathrm{L}}$  denotes load at node i in p.u.;  $P_i^{\mathrm{T}}$  and  $Q_i^{\mathrm{T}}$  are assumed to be equal to  $\sum_{j=1}^{\eta} P_{ij}^{\mathrm{line}}$  and  $\sum_{j=1}^{\eta} Q_{ij}^{\mathrm{line}}$ , respectively; such that  $P_{ij}^{\mathrm{line}}$  and  $Q_{ij}^{\mathrm{line}}$  are active and reactive power flows through the line between node i to node j in p.u.; such that if there are not any lines between nodes i and j,  $P_{ij}^{\mathrm{line}}$  and  $Q_{ij}^{\mathrm{line}}$  are equal to zero.  $P_i^{\mathrm{T}}$  and  $Q_i^{\mathrm{T}}$  can be expended as follows:

$$P_{i}^{T} = |V_{i}| \sum_{j=1}^{\eta} |V_{j}| (G_{ij} \cos(\theta_{i} - \theta_{j}) + B_{ij} \sin(\theta_{i} - \theta_{j})),$$

$$Q_{i}^{T} = |V_{i}| \sum_{j=1}^{\eta} |V_{j}| (-B_{ij} \cos(\theta_{i} - \theta_{j}) + G_{ij} \sin(\theta_{i} - \theta_{j})).$$
(2)

where  $|V_i|$  and  $\theta_i$  represent magnitude and angle of voltage at node i;  $G_{ij}$  and  $B_{ij}$  are the real and imaginary parts, respectively, of the admittance matrix  $Y_{ij} = G_{ij} + jB_{ij}$ . As  $\sin(\theta_i - \theta_j)$  is small, and the voltage is near 1.0 per unit,  $|V_i||V_j|\sin(\theta_{ij})$  can be replaced by  $\theta_{ij}$ , where  $\theta_i - \theta_j = \theta_{ij}$ . Equation (2) can be modified as follows:

$$P_{i}^{T} = G_{ii}|V_{i}|^{2} + \sum_{j=1, j\neq i}^{\eta} \left(B_{ij}(\theta_{ij}) + |V_{i}||V_{j}|G_{ij}\cos(\theta_{ij})\right),$$

$$Q_{i}^{T} = -B_{ii}|V_{i}|^{2} + \sum_{j=1, i\neq i}^{\eta} \left(G_{ij}(\theta_{ij}) - |V_{i}||V_{j}|B_{ij}\cos(\theta_{ij})\right).$$
(3)

The nonlinear term of (3),  $|V_i||V_j|\cos(\theta_{ij})$ , can be linearized using the active and reactive loss equations of lines as follows:

$$P_{ij}^{\text{loss}} = -G_{ij}|V_i|^2 - G_{ij}|V_j|^2 + 2|V_i||V_j|G_{ij}\cos(\theta_{ij})),$$

$$Q_{ii}^{\text{loss}} = B_{ij}|V_i|^2 + B_{ij}|V_j|^2 - 2|V_i||V_j|B_{ij}\cos(\theta_{ij}).$$
(4)

where  $P_{ij}^{\rm loss}$  and  $Q_{ij}^{\rm loss}$  are the real and reactive power losses of the line between nodes i and j. Subsequently, the equivalent term of  $|V_i||V_j|\cos(\theta_{ij})$  is derived from (4) for both active and reactive line power flow in the following manner:

$$|V_{i}||V_{j}|\cos(\theta_{ij}) = \left(|V_{i}|^{2} + |V_{j}|^{2} + P_{ij}^{loss}/G_{ij}\right)/2,$$

$$|V_{i}||V_{j}|\cos(\theta_{ij}) = \left(|V_{i}|^{2} + |V_{j}|^{2} - Q_{ij}^{loss}/B_{ij}\right)/2.$$
(5)

The power flow equation is adjusted by inserting (5) into (3). Furthermore, in accordance with the network's admittance matrix, the  $G_{ii}$  and  $B_{ii}$  are defined as follows, respectively:

$$G_{ii} = -\sum_{j=1, j \neq i}^{\eta} G_{ij} , \quad B_{ii} = -\sum_{j=1, j \neq i}^{\eta} B_{ij}.$$
 (6)

Therefore, equations (3) can be modified as follows:

$$P_{i}^{T} = \left(G_{ii} + \sum_{j=1, j \neq i}^{\eta} \frac{G_{ij}}{2}\right) |V_{i}|^{2} + \sum_{j=1, j \neq i}^{\eta} \left(B_{ij}(\theta_{ij}) + \left(\frac{G_{ij}|V_{j}|^{2} + P_{ij}^{loss}}{2}\right)\right)$$

$$= \frac{G_{ii}|V_{i}|^{2}}{2} + \sum_{j=1, j \neq i}^{\eta} \left(B_{ij}(\theta_{ij}) + G_{ij}\left(\frac{|V_{j}|^{2}}{2} + \frac{P_{ij}^{loss}}{2G_{ij}}\right)\right),$$

$$Q_{i}^{T} = -\left(B_{ii} + \sum_{j=1, j \neq i}^{\eta} \frac{B_{ij}}{2}\right) |V_{i}|^{2} + \sum_{j=1, j \neq i}^{\eta} \left(G_{ij}(\theta_{ij}) - \left(\frac{B_{ij}|V_{j}|^{2} + Q_{ij}^{loss}}{2}\right)\right)$$

$$= -\frac{B_{ii}|V_{i}|^{2}}{2} + \sum_{j=1, j \neq i}^{\eta} \left(G_{ij}(\theta_{ij}) - B_{ij}\left(\frac{|V_{j}|^{2}}{2} - \frac{Q_{ij}^{loss}}{2B_{ij}}\right)\right).$$
(7)

To linearize  $|V_i|^2$ ,  $f(|V_i|)$  is defined as (8). Following the principles of the Taylor series, the approximation for  $|V_i|^2$  is as follows [14]:

$$f(V_i) = |V_i|^2 \to f(|V_i|) \cong f(1) + \frac{df}{d|V_i|} \Big|_{|V_i|=1} . (|V_i| - 1),$$

$$|V_i|^2 \cong 1 + 2(|V_i| - 1) = 2|V_i| - 1.$$
(8)

Applying the Taylor approximation and considering (6) equalities in (8), the power flow equations are modified as follows:

$$P_{i}^{T} = G_{ii}|V_{i}| + \sum_{j=1, j \neq i}^{\eta} \left(B_{ij}(\theta_{ij}) + G_{ij}|V_{j}| + \frac{P_{ij}^{loss}}{2}\right)$$

$$= G_{ii}|V_{i}| - B_{ii}\theta_{i} + \sum_{j=1, j \neq i}^{\eta} \left((-B_{ij}\theta_{j}) + G_{ij}|V_{j}| + \frac{P_{ij}^{loss}}{2}\right),$$

$$Q_{i}^{T} = -B_{ii}|V_{i}| + \sum_{j=1, j \neq i}^{\eta} \left(G_{ij}(\theta_{ij}) - B_{ij}|V_{j}| + \frac{Q_{ij}^{loss}}{2}\right)$$

$$= -B_{ii}|V_{i}| - G_{ii}\theta_{i} + \sum_{j=1, j \neq i}^{\eta} \left((-G_{ij}\theta_{j}) - B_{ij}|V_{j}| + \frac{Q_{ij}^{loss}}{2}\right).$$
(9)

Assuming a network admittance matrix,  $\mathbf{Y} = \mathbf{G} + j\mathbf{B}$ , the equations in (9) are modified to matrix forms as follows:

$$\begin{bmatrix} P_{1}^{T} \\ \vdots \\ P_{\eta}^{T} \end{bmatrix} = \mathbf{G} \begin{bmatrix} |V_{1}| \\ \vdots \\ |V_{\eta}| \end{bmatrix} - \mathbf{B} \begin{bmatrix} \theta_{1} \\ \vdots \\ \theta_{\eta} \end{bmatrix} + \Psi \begin{bmatrix} P_{1}^{loss} \\ \vdots \\ P_{\eta}^{loss} \end{bmatrix},$$

$$\begin{bmatrix} Q_{1}^{T} \\ \vdots \\ Q_{\eta}^{T} \end{bmatrix} = -\mathbf{B} \begin{bmatrix} |V_{1}| \\ \vdots \\ |V_{\eta}| \end{bmatrix} - \mathbf{G} \begin{bmatrix} \theta_{1} \\ \vdots \\ \theta_{\eta} \end{bmatrix} + \Psi \begin{bmatrix} Q_{1}^{loss} \\ \vdots \\ Q_{\eta}^{loss} \end{bmatrix}.$$

$$(10)$$

# B. Linear Optimization Problem

1) Objective Function: The optimization problem is defined to minimize the load curtailment in each scenario. All decision variables are calculated based on the objective function as follows:

Objective function : 
$$P_{\text{grid}}^{\text{LC}} = \min \sum_{i=1}^{\eta} P_i^{\text{LC}},$$
 (11)

where  $P_i^{\rm LC}$  and  $P_{\rm grid}^{\rm LC}$  presents the load curtailment at node i and grid, respectively.  $P_i^{\rm LC}$  is the decision variable. The operational constraints are described in the following sections.

2) Power Flow and Lines: The constraints of the MILP problem are subjected to the following:

$$P_i^{\text{sub}} + P_i^{\text{IBR}} + P_i^{\text{LC}} - P_i^{\text{L}} - P_i^{\text{T}} = 0,$$
 (12a)

$$Q_i^{\text{sub}} + Q_i^{\text{IBR}} + Q_i^{\text{LC}} - Q_i^{\text{L}} - Q_i^{\text{T}} = 0,$$
 (12b)

$$0 \le P_i^{\text{sub}} \le P_i^{\text{sub,max}}, \quad 0 \le Q_i^{\text{sub}} \le Q_i^{\text{sub,max}}, \quad (12c)$$

$$|P_{ij}^{\text{line}}| \le P_{ij}^{\text{line,max}}, \quad |Q_{ij}^{\text{line}}| \le Q_{ij}^{\text{line,max}}, \quad (12d)$$

$$V_i^{\min} \le |V_i| \le V_i^{\max}, \quad \theta_i$$
: unrestricted, (12e)

$$0 \le P_i^{\text{LC}} \le P_i^{\text{L}}, \quad Q_i^{\text{LC}} = P_i^{\text{LC}} \left(\frac{Q_i^{\text{L}}}{P_i^{\text{L}}}\right).$$
 (12f)

where  $P_i^{\text{sub}}$ ,  $Q_i^{\text{sub}}$ ,  $P_i^{\text{IBR}}$ ,  $Q_i^{\text{IBR}}$  are decision variables.

3) ZIP loads: The load can be modeled as follows,

$$P_{i}^{L} = \hat{P}_{i}^{L} \left( \rho_{Z}^{P} (1 + 2(|V_{i}| - |\hat{V}_{i}|)) + \rho_{I}^{P} (\frac{|V_{i}|}{|\hat{V}_{i}|}) + \rho_{P}^{P} \right),$$

$$Q_{i}^{L} = \hat{Q}_{i}^{L} \left( \rho_{Z}^{Q} (1 + 2(|V_{i}| - |\hat{V}_{i}|)) + \rho_{I}^{Q} (\frac{|V_{i}|}{|\hat{V}_{i}|}) + \rho_{P}^{Q} \right),$$
(13)

where the coefficients  $\rho_{\mathcal{Z}}^{(.)}$ ,  $\rho_{\mathcal{L}}^{(.)}$ , and  $\rho_{\mathcal{P}}^{(.)}$  pertain to constant impedance, constant current, and constant power, respectively;  $|\hat{V}_i|$  represents the voltage at the base loads  $\hat{P}_i^{\rm L}$  and  $\hat{Q}_i^{\rm L}$ .  $|V_i|$  is decision variable.

4) Inverters and Droop Control: The droop control model and its curves are typically used to determine the best course of action from inverters. Here, a Q/V droop curves is considered where  $Q_i^{\rm IBR}$  is depend on  $|V_i|$  or  $\Delta |V_i|$ . The Q/V droop curve is modeled as follows [15], [16]:

$$|V_i| = |V_i^{\text{set}}| - \mathcal{K}_{Q,i}^{\text{IBR}} Q_i^{\text{IBR}}, \tag{14a}$$

$$S_i^{\mathrm{IBR,min}} \leq S_i^{\mathrm{IBR}} \leq S_i^{\mathrm{IBR,max}}, \ S_i^{\mathrm{IBR}^2} = P_i^{\mathrm{IBR}^2} + Q_i^{\mathrm{IBR}^2}, \ (14b)$$

$$V_i^{\min} \le |V_i| \le V_i^{\max}, \ V_i^{\min} \le |V_i^{\text{set}}| \le V_i^{\max},$$
 (14c)

$$\mathcal{K}_{Q,i}^{\text{IBR,min}} \le \mathcal{K}_{Q,i}^{\text{IBR}} \le \mathcal{K}_{Q,i}^{\text{IBR,max}},$$
 (14d)

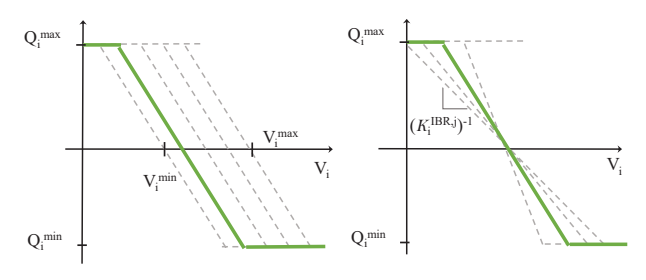


Fig. 1. Adaptive droop control: set-point (left) and injection rate (right).

where  $|V_i^{\rm set}|$  is the decision variable for the inverter at node i.  $\mathcal{K}_{Q,i}^{\rm IBR}$  represents the Q/V droop gain that is an integer decision variable, where a big-M method is applied to linearize (14a) described in Section II-B6.

5) Linearizing IBR Power Constraints: To linearize (14b), the following constraints can be defined such that an octagon shape is constructed:

$$-S_{i}^{\mathrm{IBR,max}}\cos{(\frac{\alpha}{2})} \leq P_{i}^{\mathrm{IBR}} \leq S_{i}^{\mathrm{IBR,max}}\cos{(\frac{\alpha}{2})}, \tag{15a}$$

$$-S_{i}^{\mathrm{IBR,max}}\cos{(\frac{\alpha}{2})} \leq Q_{i}^{\mathrm{IBR}} \leq S_{i}^{\mathrm{IBR,max}}\cos{(\frac{\alpha}{2})}, \tag{15b}$$

$$-S_i^{\mathrm{IBR,max}} \; \frac{\cos(\frac{\alpha}{2})}{\cos(\alpha)} \leq Q_i^{\mathrm{IBR}} \pm P_i^{\mathrm{IBR}} \leq S_i^{\mathrm{IBR,max}} \; \frac{\cos(\frac{\alpha}{2})}{\cos(\alpha)}, \; (15\mathrm{c})$$

where  $\alpha$  is equal to  $45^{\circ}$  for the octagon. The proposed method can simulate 90% of IBRs' operation area.

6) Big-M Method: Generally, the Q/V loop of inverter droop control at node i can be modeled by (14a).  $\mathcal{K}_{Q,i}^{\mathrm{IBR}}$  is an integer decision variable including d intervals such that  $\mathcal{K}_{Q,i}^{\mathrm{IBR}} \in \{\mathcal{K}_{Q,i}^{\mathrm{IBR,1}}, \dots, \mathcal{K}_{Q,i}^{\mathrm{IBR,d}}\}$  (Fig. 1). If the reactive power supplied by the inverter-based resource reaches its minimum or maximum capacity, it will not restrict the node voltage,  $|V_i|$ . Consequently, the node voltage may deviate from the values defined in the Q/V loop equation used in droop control. In other words,

$$\begin{cases} \text{if } Q_i^{\text{IBR,min}} < Q_i^{\text{IBR}} < Q_i^{\text{IBR,max}} \Rightarrow |V_i| = |V_i^{\text{set}}| - \mathcal{K}_{Q,i}^{\text{IBR,grd}} \ \text{otherwise} \\ \text{if } Q_i^{\text{IBR}} = Q_i^{\text{IBR,min}} \Rightarrow |V_i| \geq |V_i^{\text{set}}| - \mathcal{K}_{Q,i}^{\text{IBR}} \ Q_i^{\text{IBR,min}} \\ \text{if } Q_i^{\text{IBR}} = Q_i^{\text{IBR,max}} \Rightarrow |V_i| \leq |V_i^{\text{set}}| - \mathcal{K}_{Q,i}^{\text{IBR}} \ Q_i^{\text{IBR,max}} \end{cases}$$

For  $Q_i^{\mathrm{IBR}}$  between  $Q_i^{\mathrm{IBR,min}}$  and  $Q_i^{\mathrm{IBR,max}}$ ,  $Q_i^{\mathrm{IBR}}$  is presented by  $Q_i^{\mathrm{IBR,grd}}$ . In a MILP problem, the relation of decision variables in constraints needs to be linear. However, equation (16) represents a nonlinear relation between decision variables  $Q_i^{\mathrm{IBR}}$  and  $\mathcal{K}_{Q,i}^{\mathrm{IBR}}$ . To address this nonlinearity for a MILP problem, the big-M method is applied to adaptive droop control constraints. To utilize the big-M method on the nonlinear constraint in (16) [17], a new artificial parameter, " $\mathcal{M}$ ", needs to be defined to represent the nonlinear constraint.  $\mathcal{M}_{Q,i}^{\mathrm{IBR,j}}$  is defined for IBR at node i for  $j^{\mathrm{th}}$  interval,  $\mathcal{K}_{Q,i}^{\mathrm{IBR,j}}$ , as follows:

$$\bar{\mathcal{M}}_{Q,i}^{\mathrm{IBR,j}} \Gamma_{Q,i}^{j} \leq |V_{i}| - |V_{i}^{\mathrm{set}}| + \mathcal{K}_{Q,i}^{\mathrm{IBR,j}} Q_{i}^{\mathrm{IBR,grd}}$$
(17a)

$$|V_i| - |V_i^{\text{set}}| + \mathcal{K}_{Q,i}^{\text{IBR,j}} Q_i^{\text{IBR,grd}} \le \mathcal{M}_{Q,i}^{+\text{IBR,j}} \Gamma_{Q,i}^j, \tag{17b}$$

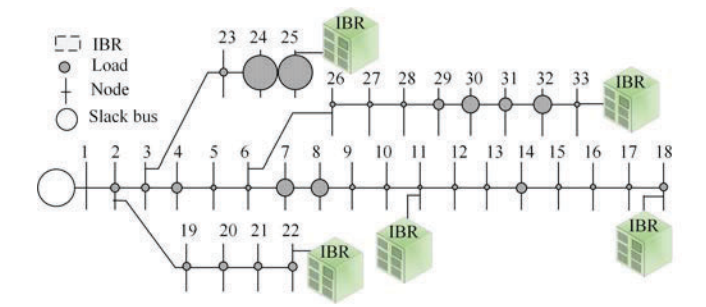


Fig. 2. IEEE 33-bus system with five droop-controlled IBRs.

$$\Gamma_{Q,i}^{j} = 1 - \psi_{i}^{j}, \quad \sum_{j=1}^{d} \psi_{i}^{j} = 1, \quad \forall \psi_{i}^{j} \in \{0, 1\},$$
(17c)

$$\mathcal{K}_{Q,i}^{\text{IBR}} = \sum_{i=1}^{d} \mathcal{K}_{Q,i}^{\text{IBR,j}} \psi_i^j, \tag{17d}$$

where  $\psi_i^j$  is the decision variable.  $\mathcal{M}_{Q,i}^{+/-}$  IBR, at node i can be determined as follows:

$$\mathcal{M}_{Q,i}^{\mathsf{IBR,j}} = \xi(V_i^{\mathrm{max}} - V_i^{\mathrm{min}}), \quad \mathcal{M}_{Q,i}^{\mathsf{IBR,j}} = \xi(V_i^{\mathrm{min}} - V_i^{\mathrm{max}}), \tag{18}$$

where  $\xi$  must be large enough.

# C. Reliability Indices

System Average Interruption Duration Index (SAIDI), System Average Interruption Frequency Index (SAIFI), and Expected Demand Not Served (EDNS) are calculated as follows, respectively:

$$SAIDI = \sum_{j=1}^{N} \frac{\mathcal{L}_{j}^{hr}}{\mathcal{L}_{j}} \times 8760 \text{ (hr/cus.yr)}, \tag{19a}$$

$$SAIFI = \sum_{j=1}^{N} \frac{\mathcal{L}_{j}^{num}}{\mathcal{L}_{j}} \times 8760 \text{ (occ/cus.yr)}, \tag{19b}$$

EDNS = 
$$\left(\sum_{i=1}^{N} P_{total,j}^{\text{LC}}\right)/N$$
 (MW), (19c)

where N is the number of scenarios;  $\mathcal{L}_{j}^{hr}$  and  $\mathcal{L}_{j}^{num}$  are the duration of sustained customer interruptions in hours and the number of sustained customer interruptions in scenario j per customer per year;  $\mathcal{L}_{j}$  is the total number of customers in scenario j; and  $P_{total,j}^{\text{LC}}$  represents the curtailment at scenario j in MW.

## III. CASE STUDY

## A. Modeling Consideration and Simulation

Fig. 2 shows a modified IEEE 33-bus system simulated to aim to test the proposed approach in this study. The IBRs in Fig. 2 are modeled as described in Section II-B4.  $\rho_{\mathcal{Z}}^{(.)}$ ,  $\rho_{\mathcal{I}}^{(.)}$ , and  $\rho_{\mathcal{P}}^{(.)}$  in ZIP load model are assumed 0.5, 0.4, and 0.1, respectively [18]. The load peak is 5.25+j3.69 MVA. The load congestion level is schematically indicated in Fig. 2 by small or large circles at each node. The main grid can supply up to 40% peak load.

 $\label{thm:table inverter-based resources.} The \ reliability information of the inverter-based resources.$ 

Node	Apparent Power (MVA)	MTTF (hr/yr)	MTTR (hr/yr)
11	1.08	8607	153
18	1.275	8603	157
22	0.75	8634	126
25	1.275	8621	139
33	0.75	8657	103

TABLE II
THE RELIABILITY INDICES FOR FOUR CASE STUDIES.

Description	SAIDI (hr/cus.yr)	SAIFI (occ/cus.yr)	EDNS (kW)
Constant control	734.09	15.45	417.23
VSP control	6.19	0.55	3.52
Adaptive control	3.09	0.37	1.76

An MILP problem is developed to conduct the reliability assessment and solved based on the objective function (11). The contingencies are generated based on the sequential Monte Carlo technique and failure rates chosen based on [19], [20] and tabulated in Table I for the IBRs.

## B. Results and Analysis

Table II reports reliability indices for the system based on the MILP problem results described in Section II. The table represents a comparison of reliability indices between three different case studies: constant droop control, voltage set-point (VSP) control, and fully optimized droop gain control of IBRs. In voltage set-point control, the droop gain is constant, and the voltage reference for droop control is variable. Incorporating adaptive droop gain in system operation, the SAIDI and SAIFI are improved by 99.57% and 97.61%, respectively, meaning the duration and number of not-supplied customers are decreased significantly.

Moreover, the improved result of voltage set-point control shows that the flexibility of voltage set-point can improve system reliability by solving the voltage regulation problem. In other words, unreliable scenarios can happen due to voltage drop in a system. Utilizing the fully optimized or voltage set-point control methods of droop control can help improve voltage regulation, specifically in long feeders, reducing the number of unsupplied customers.

To conduct a comprehensive investigation into the enhancement and consequential impact of adaptive droop control of inverters on system reliability, a node-based reliability study is provided. This study aids in elucidating the intricate aspects of system improvement when employing the advanced control methodology within the system.

Fig. 3 represents the node-based reliability indices to highlight the vulnerable nodes and local customers of the system and their effect on the system reliability. Also, Fig. 3 compares the results for three case studies, including constant droop control, voltage set-point control, and adaptive control. Comparing the voltage of the nodes (Fig. 3-(d)) shows that the adaptive droop control improves the voltage profile at nodes 13 to 17, which is a part of the longest feeder of the network.

The improvement of inadequacy at nodes 25 and 29 (Fig. 3-(c)) shows dependency on reactive power and voltage regu-

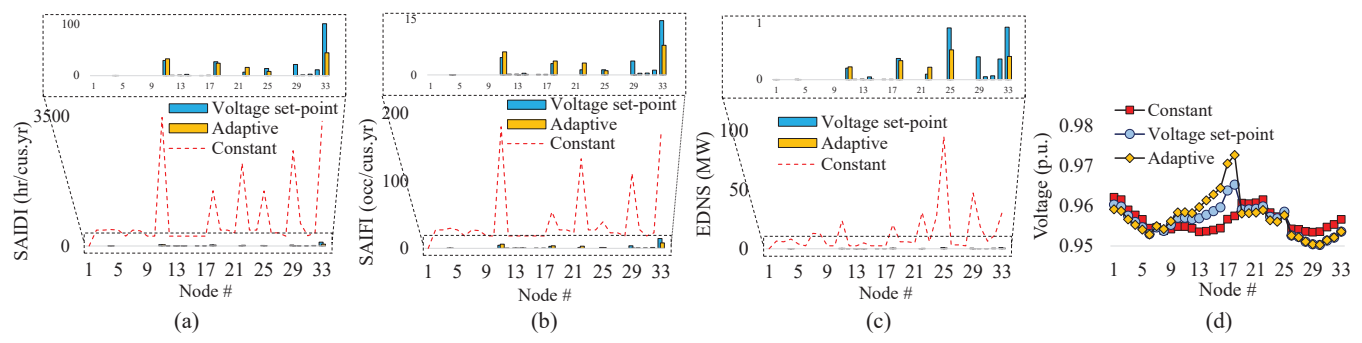


Fig. 3. (a) Local SAIDI, (b) local SAIFI, (c) local EDNS, and (d) local average voltage for three inverter control approaches.

lation such that by unlocking the voltage set-point variable of the control system, the reliability indices at these nodes are reduced significantly. Moreover, utilizing the adaptive droop gain in the control system can harness the maximum potential of system reliability to supply the customers at nodes 29, 32, and 33 (Fig. 3-(c)).

Integrating adaptive droop control in system adequacy for IBRs allows for efficient power distribution and effective management of network power. It also facilitates reactive power and voltage regulation, which are key to minimizing load curtailments and maintaining system reliability, especially with the integration of variable renewable energy sources.

#### IV. CONCLUSION

This paper has introduced an innovative approach that integrates adaptive droop control for inverter-based resources, aiming to enhance the overall reliability of the power system. By allowing for a variable droop control, this method empowers inverter-based resources to optimize their power output, thereby effectively regulating voltage levels to serve the maximum number of customers possible. An MILP problem has been formulated, utilizing a linear AC-OPF framework in conjunction with the adaptive droop gain concept, applied to a modified IEEE 33-bus system.

The results and performance indices obtained through the analysis serve as compelling evidence of the substantial positive impact of this adaptive control system for inverters on the enhancement of system reliability. Moreover, a variable voltage set-point control has determined that the unreliability of the system is not just related to inadequate generation; the voltage regulation problem can be one of the most important reasons for system failures and unsupplied customers.

## ACKNOWLEDGEMENT

This work was supported in part by the U.S. National Science Foundation (NSF) under Grant 1847578.

## REFERENCES

- [1] P. Zhang, W. Li, S. Li, Y. Wang, and W. Xiao, "Reliability assessment of photovoltaic power systems: Review of current status and future perspectives," *Applied energy*, vol. 104, pp. 822–833, 2013.
- [2] S. Kennedy, "Reliability evaluation of islanded microgrids with stochastic distributed generation," in 2009 IEEE Power & Energy Society General Meeting. IEEE, 2009, pp. 1–8.

- [3] I.-S. Bae and J.-O. Kim, "Reliability evaluation of distributed generation based on operation mode," *IEEE Trans. Power Syst*, vol. 22, no. 2, pp. 785–790, 2007.
- [4] Y. Atwa, E. F. El-Saadany, M. Salama, R. Seethapathy, M. Assam, and S. Conti, "Adequacy evaluation of distribution system including wind/solar dg during different modes of operation," *IEEE Trans. Power Syst*, vol. 26, no. 4, pp. 1945–1952, 2011.
- [5] R. Karki and R. Billinton, "Reliability/cost implications of pv and wind energy utilization in small isolated power systems," *IEEE Transactions* on Energy Conversion, vol. 16, no. 4, pp. 368–373, 2001.
- [6] Z. Bie, P. Zhang, G. Li, B. Hua, M. Meehan, and X. Wang, "Reliability evaluation of active distribution systems including microgrids," *IEEE Trans. Power Syst*, vol. 27, no. 4, pp. 2342–2350, 2012.
- [7] I.-S. Bae and J.-O. Kim, "Reliability evaluation of customers in a microgrid," *IEEE Trans. Power Syst*, vol. 23, no. 3, pp. 1416–1422, 2008.
- [8] M. Al-Muhaini and G. T. Heydt, "Evaluating future power distribution system reliability including distributed generation," *IEEE Transactions* on Power Delivery, vol. 28, no. 4, pp. 2264–2272, 2013.
- [9] H. Hosseinpour and M. Benidris, "An integrated adequacy and stability assessment approach for microgrid reliability analysis," *Available at* SSRN 4624977.
- [10] M. Fotuhi-Firuzabad and A. Rajabi-Ghahnavie, "An analytical method to consider dg impacts on distribution system reliability," in *IEEE PES Transmission & Distribution Conference & Exposition: Asia and Pacific*. IEEE, 2005, pp. 1–6.
- [11] M. E. Khodayar, M. Barati, and M. Shahidehpour, "Integration of high reliability distribution system in microgrid operation," *IEEE Transactions on Smart Grid*, vol. 3, no. 4, pp. 1997–2006, 2012.
- [12] S. Conti, R. Nicolosi, and S. Rizzo, "Generalized systematic approach to assess distribution system reliability with renewable distributed generators and microgrids," *IEEE Transactions on Power Delivery*, vol. 27, no. 1, pp. 261–270, 2011.
- [13] J. Mitra, "Linear optimal power flow system and method," May 21 2019, US Patent 10,296,988.
- [14] A. Safdarian, M. Fotuhi-Firuzabad, F. Aminifar, and M. Lehtonen, "A new formulation for power system reliability assessment with ac constraints," *International Journal of Electrical Power & Energy Systems*, vol. 56, pp. 298–306, 2014.
- [15] R. Sadnan and A. Dubey, "Distributed optimization in distribution systems with grid-forming and grid-supporting inverters," in *IEEE Power & Energy Society General Meeting*. IEEE, 2022, pp. 01–05.
- [16] M. MansourLakouraj, H. Hosseinpour, H. Livani, M. Benidris, and M. S. Fadali, "Volt/var support and demand response co-optimization in distribution systems with adaptive droop control of inverters," in *IEEE Texas Power and Energy Conferenc*, 2023, pp. 1–6.
- [17] R. A. Jabr, "Economic operation of droop-controlled ac microgrids," IEEE Trans. Power Syst, vol. 37, no. 4, pp. 3119–3128, 2021.
- [18] M. MansourLakouraj, H. Livani, and M. Benidris, "Risk-averse scheduling via conservation voltage reduction in unbalanced distribution feeders," in *IEEE Texas Power and Energy Conference*, 2022, pp. 1–6.
- [19] C. Singh and J. Mitra, "Monte carlo simulation for reliability analysis of emergency and standby power systems," in IAS'95. Conference Record of the 1995 IEEE Industry Applications Conference Thirtieth IAS Annual Meeting, vol. 3. IEEE, 1995, pp. 2290–2295.
- [20] C. Singh, P. Jirutitijaroen, and J. Mitra, Electric power grid reliability evaluation: models and methods. John Wiley & Sons, 2018.